Temperature Dependence of Inversion-Layer Frequency Response in Silicon

By A. GOETZBERGER and E. H. NICOLLIAN

(Manuscript received October 28, 1966)

Conductance-voltage and capacitance-voltage curves of metal-oxide semiconductor (MOS) capacitors on n-type silicon were investigated in the temperature range between room temperature and 200°C. Plots of the inversion-layer conductance versus reciprocal temperature show a sequence of two activation energies: one corresponding to the temperature dependence of the intrinsic carrier density n_i , the other to that of n_i^2 . The low-temperature range is characterized by recombination-generation in the space-charge region, the high-temperature range by diffusion current from the bulk. The technique permits measurement of bulk lifetime for the two regimes and determination of room temperature cutoff frequency for the channel.

I. INTRODUCTION

Theoretical calculations of metal-oxide semiconductor (MOS) capacitance show a total capacitance approaching oxide capacitance in strong accumulation and strong inversion.[1] Experimentally, it has been found that response time of the inversion layer can be very long.[2] The response time can be drastically shortened, however, by lateral ac current flow in an extended inversion layer.[2,3] The lateral current flow mode requires equilibrium surface inversion beyond the metal contact. This condition is usually found in p-type silicon because of the preponderance of positive surface charge in thermally oxidized silicon. Channel cutoff frequencies are then typically in the MHz range.

In n-type silicon, charge in the inversion layer can communicate with the bulk under steady-state conditions only by means of generation-recombination processes.[2] Inversion-layer cutoff frequencies in n-type silicon are normally below 100 Hz, sometimes below 1 Hz. These low frequencies make it difficult to measure cutoff frequencies and to determine the mechanism of generation of minority carriers.

In this study, measurements with n-type silicon were carried out at elevated temperature where generation is more rapid. It is thus possible to study the generation mechanisms and confirm the theory for calculating response time. This theory was derived by Hofstein and Warfield.[2] They consider three different generation mechanisms for minority carriers. These are: bulk diffusion current, space-charge generation, and surface-state generation. Fig. 1 shows a simplified equivalent circuit proposed by Hofstein and Warfield for strong inversion. The inversion capacitance is fed by three parallel conductances corresponding to the three generation mechanisms. Because inversion capacitance is large compared to oxide capacitance with which it is in series, it can be neglected as done in Fig. 1.

The conductances are given for n-type bulk material by the following relations.[2]

For surface-state response

$$G_{g,s} = q\beta N_s N_D e^{\beta\psi_s} \sigma_p v_p , \tag{1}$$

where q = electronic charge in coulombs, N_s = surface-state density/cm^2, N_D = donor density in the bulk in cm^{-3}, $\beta = q/kT$, σ_p = capture cross section for holes in cm^2, v_p = average thermal velocity of holes in cm/sec, and ψ_s = surface potential in volts. Relation (1) was originally derived for a single level close to midgap. Because only levels in this range contribute to recombination, it is also valid for a continuum of surface states as is generally encountered in oxidized surfaces.

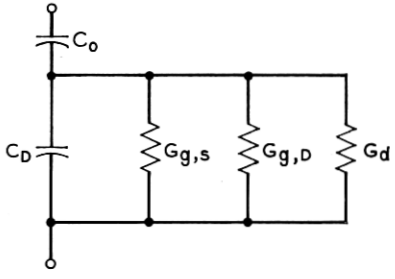

Fig. 1—Equivalent circuit of MIS capacitor in strong inversion proposed in Ref. 2. C_o is the oxide layer capacitance per cm^2, C_D is the depletion layer capacitance per cm^2, $G_{g,s}$ is the conductance arising from generation-recombination through surface states, mhos/cm^2, $G_{g,D}$ is the conductance arising from generation-recombination through states in the silicon space-charge region, mhos/cm^2, and G_d is the conductance due to the diffusion of minority carriers from the quasi neutral region in the silicon to its surface, mhos/cm^2.

Space-charge generation response:

$$G_{g,D} = \frac{qn_i\, d}{\tau_o \psi_s}, \tag{2}$$

where n_i = intrinsic carrier density in cm^{-3}, τ_o = bulk lifetime in seconds, and d = space-charge layer thickness in cm.

Diffusion response

$$G_d = \frac{q\mu_p n_i^2}{L_p N_D}, \tag{3}$$

where μ_p = hole mobility in cm^2/volt-sec, and L_p = diffusion length for holes in cm. We have further

$$L_p = (\tau_o \mu_p/\beta)^{\frac{1}{2}}. \tag{4}$$

By measuring temperature dependence of the inversion-layer response, it is possible to determine which mechanism is dominant. Surface-state generation should go with an activation energy of ψ_s. It has to be considered here that ψ_s is itself a function of temperature. Space-charge generation has the activation energy of n_i, and diffusion current that of n_i^2. In the present investigation, surface-state density was made very small, so that only $G_{g,D}$ and G_d had to be considered. This was also done because surface-state density can reach high values close to the band edges.[4,5] This, in turn, causes considerable uncertainty of the value of surface potential. In the absence of surface-state effects, the experiments reported here showed that at low temperature space-charge generation dominates while at higher temperature diffusion current takes over.

II. EXPERIMENTAL TECHNIQUE

Samples used for the measurements consisted of expitaxial layers of 1.5×10^{16} cm^{-3} doping, 10 μ thick, on low-resistivity substrates of [100] orientation. Use of epitaxial samples was advantageous because the measurements were not affected by series resistance in the substrate. Because epitaxial layers are not as perfect as regular crystals, rather low lifetimes were encountered. Samples were thermally oxidized in steam to a thickness of 1000 Å. The previously described bias oxidation technique[6] was used. In order to reduce surface-state density, the samples were subjected to a 30-minute annealing treatment in N_2 at 350°C after an aluminum film had been evaporated.[7,8] After annealing, circular areas of 3.75×10^{-2} cm diameter were etched out for MOS measurements. Capacitance and conductance were measured versus voltage

at 100 KHz and 6 KHz at various temperatures. For this purpose, the entire wafer was placed on a heated stage and contact was made to one capacitor with a wire probe. Temperature was controlled to $\pm 2°C$. Next, depletion-layer capacitance and inversion-layer conductance were extracted from the raw data by correcting for oxide capacitance as described in Ref. 5 and 3.

III. RESULTS

A family of capacitance versus voltage curves and conductance versus voltage curves at 6 KHz are shown in Figs. 2 and 3. Figs. 4 and 5 contain 100-KHz curves for the same sample. It is seen that both capacitance and conductance saturate in the inversion range at negative voltage. Due to the influence of the residual surface-state density small bumps appear in the depletion region. In Figs. 6 and 7, Arrhenius plots of the computed inversion conductance G_I are presented. These curves were obtained from the conductance curves of Figs. 3 and 5

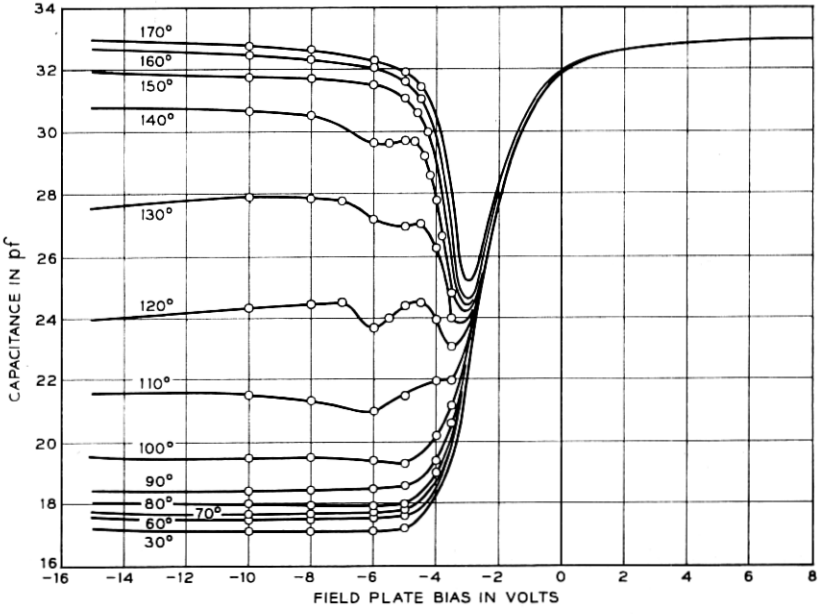

Fig. 2 — Capacitance vs field plate bias measured at 6 kHz with temperature in °C as parameter. Sample is n-type silicon oriented in the [100] direction. Field plate diameter is 370 μ, donor density is 1.17×10^{16} cm^{-3}, and oxide layer capacitance is 2.84×10^{-7} farads/cm^2.

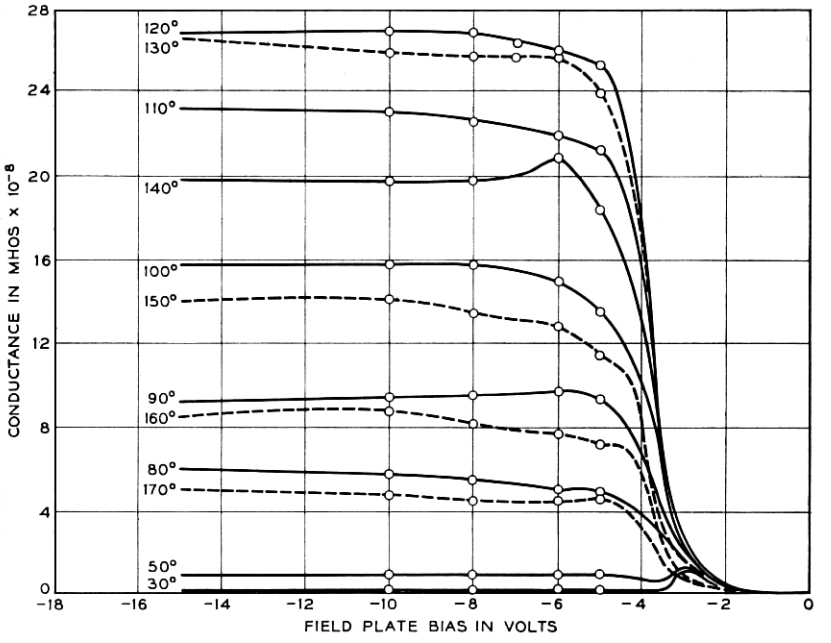

Fig. 3—Equivalent parallel conductance vs field plate bias measured at 6 kHz with temperature in °C as parameter. Sample is the same as in Fig. 2. Conductance is peaked at 120°C. Dotted lines are on high and solid lines on low-temperature side of peak.

at high negative voltage. The fact that both plots agree within the accuracy of the measurement indicates that the equivalent circuit of Fig. 1 is valid. The values of the activation energies also prove that in the surface studied here there is no noticeable influence from surface states. Fig. 8 contains room temperature capacitance-voltage curves at various frequencies.

IV. DISCUSSION

Hofstein and Warfield[2] showed that the dominant effect is most likely space-charge recombination (2). Surface recombination may also be important at relatively high surface-state densities. Because the sample investigated here contained very few surface states, it can be expected that space-charge recombination dominates. From Fig. 6 it is seen that this is the case up to temperatures around 140°C. In this range, the activation energy is 0.56 eV for Fig. 6, curve (a), and

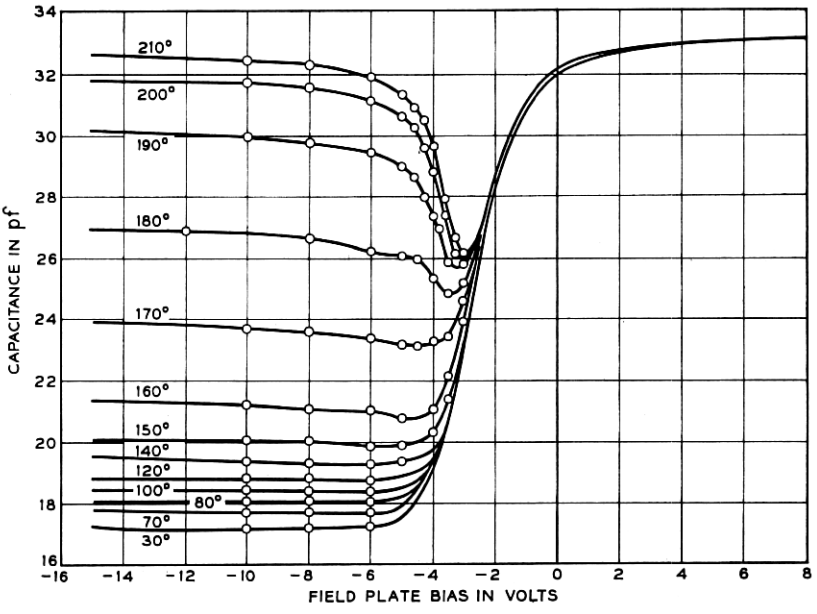

Fig. 4—Capacitance vs field plate bias measured at 100 kHz with temperature in °C as parameter. Sample is same as in Fig. 2.

0.620 eV for Fig. 7, curve (a). The expected activation energy[9] for n_i is 0.605 eV. Equation (2) can now be used to calculate bulk lifetime, τ_o, under certain simplifying assumptions given in Ref. 2. We obtain $\tau_o = 4.19 \times 10^{-9}$ seconds. This rather low lifetime is explained by the fact that it refers to an epitaxial layer.

Above 140°C a new process dominates as shown by the break in the $1/T$ curves. This process could be either surface-state generation or diffusion current from the neutral part of the bulk. It can be shown that surface-state generation is very unlikely in this case. Surface-state density as determined by the conductance technique[5] is varying between 6.1×10^{10} and 3.3×10^{11} states per cm^2 and eV. This density would, according to (1), give a conductance orders of magnitude lower than the measured G_I. It is also expected that the activation energy of surface-state processes should decrease because surface potential at constant voltage decreases considerably with increasing temperature.

If the high-temperature points in Figs. 6 and 7 are connected by a straight line, they give an activation energy of 0.908 eV for 6 KHz and 0.935 eV for 100 KHz. This energy is lower than the expected energy of 1.21 eV. The discrepancy can be resolved by correcting the

high temperature points by subtracting the influence of space-charge generation as indicated in Fig. 6, curve (*c*). If this is done, the high-temperature activation energy in Fig. 6, curve (*c*), is 1.17 eV which is very close to the expected value. Fig. 7 did not contain sufficient experimental points to carry out the correction.

Using (3) and (4), the high-temperature lifetime and diffusion length can be calculated. We find, $L_p = 20.1\ \mu$ and $\tau_o = 1.8 \times 10^{-7}$ seconds. Because the calculated diffusion length is of the order of the epitaxial layer thickness, it is possible that the actual diffusion length might be longer. In calculating the above values, a temperature dependence of the mobility μ_p of $T^{\frac{1}{2}}$ was used as is necessary for highly-doped samples.

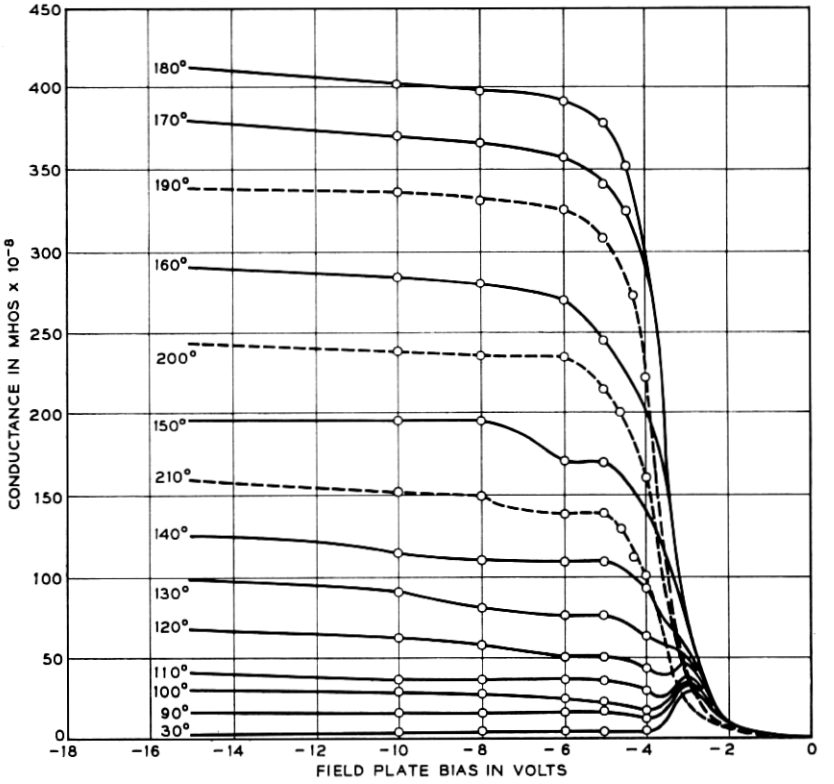

Fig. 5—Equivalent parallel conductance vs field plate bias measured at 100 kHz with temperature in °C as parameter. Sample is same as in Fig. 2. Conductance is peaked at 180°C. Dotted lines are on high and solid lines are on low-temperature side of peak.

The two lifetimes calculated from the two temperature ranges are actually expected to be equal. The linearity of the plots in curve (*b*) of Figs. 6 and 7 indicates that there is no great temperature dependence of τ_o. A possible explanation for the discrepancy of lifetimes is that they are measured in different parts of the crystal. Space-charge recombination occurs within 0.5 μ from the surface, while diffusion lifetime is determined in the entire epitaxial layer. It is likely that a thin surface layer contains a higher concentration of recombination centers.

An alternative explanation is that electron and hole lifetime are

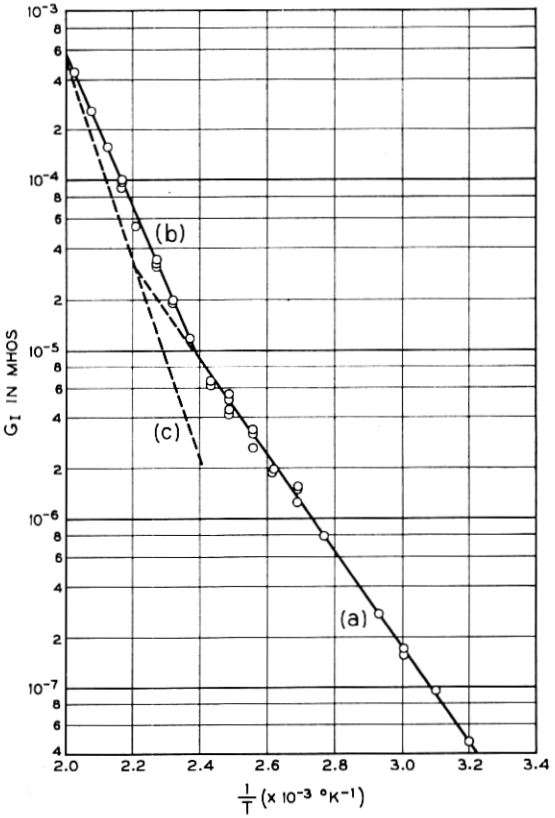

Fig. 6—Equivalent parallel conductance measured at 6 kHz and a bias of −15 volts as a function of reciprocal degrees Kelvin. The experimental points indicated by the circles were obtained from Fig. 3. Multiple circles at a given temperature represent several runs. The solid lines are the best fit to the experimental points. Curve (*c*) is obtained by subtracting the values of G_I in curve (*b*) from the extrapolation of curve (*a*) at each temperature.

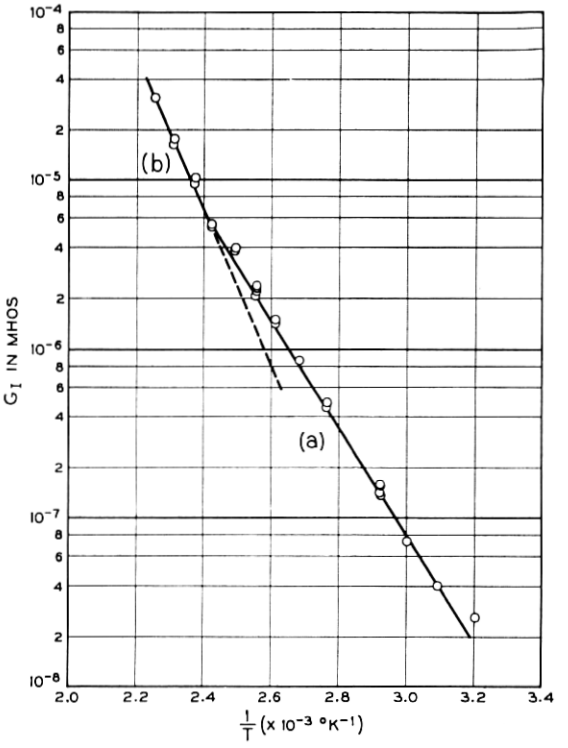

Fig. 7 — Equivalent parallel conductance measured at 100 kHz and a bias of −15 volts as a function of reciprocal degrees Kelvin. The experimental points indicated by the circles were obtained from Fig. 5. Multiple circles at a given temperature represent several runs. The solid lines are the best fit to these points.

significantly different. In this case, $\tau_o = (\tau_{no}\tau_{po})^{\frac{1}{2}}$ would have to be used in (2) and $\tau_o = \tau_{po}$ in (3). Under this assumption τ_{no} is calculated to be 10^{-10} second.

By taking inversion conductance from the curves in Fig. 6 at room temperature, inversion-layer time constant can be accurately calculated. This time constant[2] is $\tau_I = C_D/G_I = 2.25 \times 10^{-3}$ second leading to a cutoff frequency of 71 Hz. Fig. 8 demonstrates that a cutoff frequency in this neighborhood is indeed observed.

V. CONCLUSIONS

By measuring inversion conductance, it could be shown that the equivalent circuit and theory by Hofstein and Warfield is valid. The

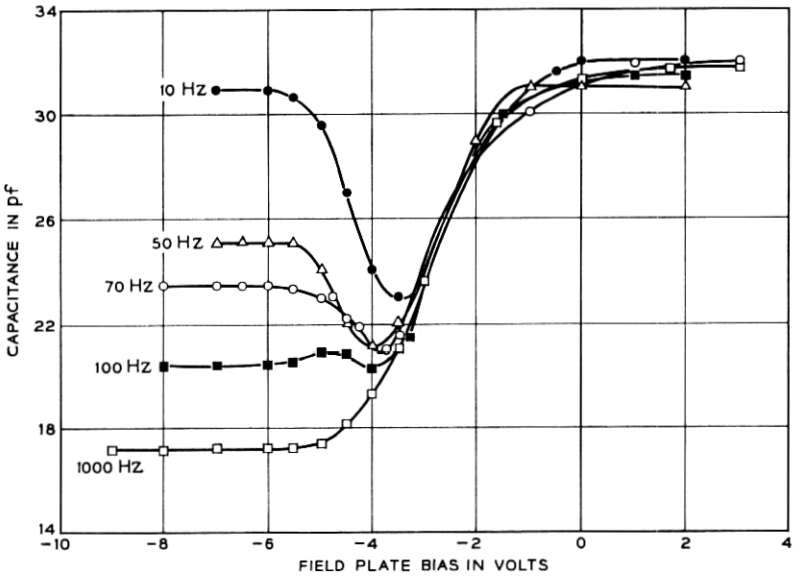

Fig. 8—Capacitance vs field plate bias measured at 27°C with frequency as parameter. Sample is the same as in Fig. 2.

technique applied here permits an estimate of the room-temperature time constant of an inversion layer by extrapolating the high-temperature curves. This way, even very long time constants may be estimated. In samples having low surface-state density, like the one described here, only bulk generation processes are important. The temperature range up to 140°C is characterized by space-charge generation, above this range diffusion current which has a higher activation energy becomes more important.

VI. ACKNOWLEDGMENT

We wish to thank R. V. Terio for his help in making the measurements.

REFERENCES

1. Lindner, R., Semiconductor Surface Varactor, B.S.T.J., *41*, 1962, p. 803.
2. Hofstein, S. R. and Warfield, G., Solid-State Electron, *8*, 1965, p. 321.
3. Nicollian, E. H. and Goetzberger, A., IEEE Trans., *ED-12*, 1965, p. 108.
4. Grey, P. V. and Brown D. M., Appl. Phys. Letters, *8*, 1966, p. 31.
5. Nicollian, E. H. and Goetzberger, A., to be published.
6. Goetzberger, A., J. Electrochem. Soc., *113*, 1966, p. 138.
7. Balk, P., Electrochem. Soc. (Extended Abstracts, Electronics Division), *14*, 1965, p. 237,
8. Goetzberger, A. and Nigh, H. E., Proc. IEEE, *54*, 1966, p. 1454.
9. Morin, F. J. and Maita, J. P., Phys. Rev., *94*, 1954, p. 1525.